Natural demodulation of two-dimensional fringe patterns: I.

General background of the spiral phase quadrature transform.

Kieran G. Larkin*, Donald J. Bone†, and Michael A. Oldfield.

Canon Information Systems Research Australia Pty Ltd, 1 Thomas Holt Drive, North Ryde, Sydney, NSW 2113, Australia.

†Advanced Image Research, P.O. Box 1001, Dickson ACT 2602, Australia.

*Also at Department of Physical Optics, School of Physics, The University of Sydney, NSW 2006, Australia.

Abstract

It is widely believed, in the areas of optics, image analysis and visual perception, that the Hilbert transform does not extend naturally and isotropically beyond one dimension. In some areas of image analysis this belief has restricted the application of the analytic signal concept to multiple dimensions. We show that contrary to this view there is a natural, isotropic and elegant extension. We develop a novel two-dimensional transform in terms of two component parts: a spiral phase spectral (Fourier) operator combined with an orientational phase spatial operator. Combining the two operators results in a meaningful two-dimensional quadrature (or Hilbert) transform. The new transform is applied to the problem of closed fringe pattern demodulation in two dimensions, resulting in a direct solution. The new transform has connections with the Riesz transform of classical harmonic analysis. We consider these connections, as well as connections with the propagation of optical phase singularities and the reconstruction of geomagnetic fields.

Keywords: Hilbert transform, Fourier transform, demodulation, phase, Riesz transform, quadrature transform, image analysis, spiral phase, optical vortices.

OCIS: 100.2650 Fringe analysis, 100.2960 Image analysis, 100.5070 Phase retrieval, 100.5090 Phase-only filters (kinoforms), 120.3180 Interferometry, 120.5050 Phase measurement

1. Introduction: Historical Survey

Our work on the natural demodulation of two-dimensional fringe patterns will be presented in two parts. In this, paper I, we present a background to the heuristic derivation of the spiral phase quadrature transform and some simulations. In paper II a mathematical basis for the validity and accuracy of the spiral phase quadrature transform is investigated.

To help understand the confusion regarding the extension of the Hilbert transform beyond one dimension a brief historical survey of the literature is useful.

The concept of an analytic (or holomorphic) signal was introduced to communication theory by Gabor in 1947[1] for one-dimensional (1-D) signals. An analytic signal consist of two parts: the real part is the base signal and the imaginary (or quadrature) part is the Hilbert transform of the real part. The theory of analytic signals naturally underpins many modern concepts of signal analysis such as amplitude and frequency (AM-FM) demodulation, spectral analysis, instantaneous frequency, interferometry, and radar. Unfortunately the concept has not, apparently, extended naturally beyond one dimension, without implying a preferred direction. Consequently a number of avowedly ad hoc definitions of the 2-D Hilbert transform have been proposed [2-7] with varying degrees of directionality. Typical definitions have half-plane symmetry[5], quadrant based symmetry[8, 9] or rotated half-plane symmetry.[10] A recent development is the idea of extending the complex analysis of the Fourier transform to hyper-complex numbers. The concept has been called "hyper-complex signal representation" by Bülow[11, 12], and potentially allows an unambiguous definition of the analytic image in 2-D. Unfortunately and surprisingly, the published definition has a

degree of directionality which is apparent in the demodulated envelope patterns.[11] A similar idea using quaternions and even octonions for multi-dimensional signals was proposed by Craig in 1996[13]. The quaternionic approach allows several possible definitions but introduces additional phases in the definition of the analytic image, which have no clear interpretation.

In the area of phase-retrieval the concept of analyticity is central to the understanding of multi-dimensional bandlimited signals.[14] Interestingly the mathematical development of a complex function of several complex variables (and the associated Cauchy-Riemann equations) leads, in this case, to a non-isotropic interpretation of the Hilbert transform relations in the two real space variables.[15, 16] However, an alternative definition of the multi-dimensional Cauchy-Riemann conditions leads to isotropic equations.[17] In an isotropic system it is not clear why there should be a preferred direction. Sometimes anistotropic definitions are justified by the symmetry of the problem. So for example images obtained by differential interference contrast (DIC) microscopy have one direction related to the differential shear, so the application of a directional multi-dimensional Hilbert transform may be appropriate.[18] Similarly, in 3-D white-light interferometry the Hilbert transform relation applies to just one coordinate.[19]

Little known to many researchers in signal processing, the theory of the Hilbert transform extended to n-dimensions (n real variables) has been in development since the1920s by pure mathematicians working in an area known as the harmonic analysis of singular integrals. Following Hilbert's lead[20] Marcel Riesz[21] proposed "fonctions conjuguées" or conjugate functions as extensions to the Hilbert transform. At the same time, independent work by Tricomi,[22] and Giraud[23] developed the same idea. More recently the works of Mikhlin[24, 25] followed soon after by Calderon and Zygmund[26, 27]

have proved the existence and convergence of the associated integral operators.[28] Another approach to the problem by the generalisation of the Cauchy-Riemann conditions to higher dimensions was undertaken by Fulton.[17] Readers wishing to follow the rather circuitous development of the n-dimensional Riesz transform (as the n-dimensional analogue of the Hilbert transform is now known) are advised to start with the textbooks by Stein,[29] and Mikhlin,[25] and the article by Carberry.[30] The main complication with the Riesz transform is that it is an n-vector for an n-dimensional scalar signal and it has not been apparent how to incorporate the 2-vector image into conventional image processing.

Perhaps, of all the applied sciences, geophysics has been the most successful in finding possible definitions of the 2-D Hilbert transform over the years.[13, 31-34] Indeed the definitions of Nabighian[32] and Craig[13] developed for geomagnetic field analysis coincide with the definition the Riesz transform, although they do not refer to the Reisz transform in their work.

A number of reputable researchers have claimed that a true 2-D Hilbert transform can be considered difficult[35] or impossible.[6, 36-39] The difficulty is based on the perceived problem of extending the 1-D signum function, central to the 1-D Hilbert transform, to a 2-D signum function. The spiral phase formalism for the 2-D Hilbert transform developed in this paper marks a conceptual change from the incumbent linear signum function to a revolutionary signum function. To demonstrate the power of the new formalism we use an intractable problem in fringe pattern analysis which becomes almost trivial because the usual difficulty in linearly separating spectral zones does not occur.

Two recent publications have touched on the idea of an isotropic Hilbert transform. The first[40] (written in German, but our translation is available) explicitly uses

the 2D Riesz transform to enhance digital images. The second,[41] considers a "radial Hilbert transform" for digital image enhancement but in the context of an optical spiral phase filter implemented with a spatial light modulator (SLM). Neither publication discusses the rather significant quadrature effects of the transform. In this publication we shall concentrate upon the remarkable phase and quadrature related effects rather than the intensity or magnitude effects seen in digital images.

2. Background: The one-dimensional Hilbert transform

Details of the conventional Hilbert transform H and analytic signal are well described in Bracewell's classic textbook.[42] Perhaps the most important property for signal processing is that it transforms all cosine components in a function of *x* to sines and vice versa, regardless of scale factor λ:

$$-\sin(\lambda x) = \mathrm{H}\{\cos(\lambda x)\} \; for \; \lambda > 0, \tag{1}$$

and

$$\cos(\lambda x) = \mathrm{H}\{\sin(\lambda x)\}. \tag{2}$$

In many cases the Fourier (or spectral) description of the Hilbert transform is informative:

$$\hat{f}(x) = \mathrm{H}\{f(x)\}, \tag{3}$$

defines the Hilbert transform of a real function *f*, and

$$p(x) = f(x) - i\hat{f}(x) = |b(x)| \exp[i\psi(x)], \tag{4}$$

defines the corresponding complex analytic signal.

The Fourier transform operator F, operating on a function *g* is given by

$$G(u) = \int_{-\infty}^{+\infty} g(x) \exp(2\pi i u x) dx = \mathrm{F}\{g(x)\}, \tag{5}$$

whereas the Fourier transform of the Hilbert transform of g is given by

$$i \operatorname{sign}(u) G(u) = \mathrm{F}\{\hat{g}(x)\}. \tag{6}$$

In other words the Fourier transform of the Hilbert transform of g is the Fourier transform of g multiplied by an imaginary signum function (see figure 1). Note that g and $\hat{g}$ are real functions. Many attempts to extend the Hilbert transform are based on extending the signum function to two dimensions. Conventionally these are products of 1-D functions which result in the half-plane and the quadrant signum functions. Such products are highly anisotropic owing to the directional line discontinuities, culminating in the familiar anisotropic definitions. A more promising approach, conceptually, is to maintain the point discontinuity of the 1-D signum function in higher dimensions. Clearly a point is a non-directional discontinuity in two or more dimensions. The transforms of several authors actually have a point discontinuity,[13, 32] however the output is not scalar for a scalar input, but either a 2-vector or a quaternion. It is not always clear how to interpret the output in such cases, and this may explain to some extent why these methods have not been endorsed more generally.

3. Two-dimensional quadrature functions

We are quite clear about what we demand of a 2-D quadrature transform, even if a 2-D Hilbert transform is difficult to agree upon. A classical problem in fringe analysis illustrates the requirements rather well. A typical 2-D fringe pattern has the following form:

$$f(x,y) = a(x,y) + b(x,y)\cos\left[\psi(x,y)\right]. \tag{7}$$

Typically the offset and modulation terms a and b respectively are slowly and smoothly varying functions. The phase function ψ is also smoothly varying, but the combined effect is a rapidly oscillating function f. The objective of fringe pattern analysis (also the objective of AM-FM signal demodulation in general) is to extract the amplitude and phase functions, $b(x,y)$ and $\psi(x,y)$ respectively. One of the most powerful methods – known as the Fourier Transform Method (FTM) - was originally developed for 1-D[43, 44] and subsequently extended to 2-D.[45] The two main complications in 2-D are that the FTM cannot separate the overlapping spectral components of closed curve fringes, and there are local and global ambiguities in the sign (±) of the output quadrature estimate.[46] Until now, no direct methods have been able to surmount these obstacles (note that indirect methods using either computationally intensive optimisation algorithms[47] or extensive manual intervention can succeed). We can identified two key points in the development of a direct 2-D quadrature method. The first is, in accordance with conventional belief, the definition of a suitable 2-D signum function in the spectral domain. The second is that a 2-D signum function alone is

unable to ensure that the output is real (for real input), of the correct polarity, and direction insensitive. To do this we propose a second operation purely in the spatial domain.

The full 2-D Fourier domain analysis of our proposed operator is presented in paper II. Our proposed 2-D signum function is defined simply as a pure spiral phase function in spatial frequency space (u,v):

$$S(u,v) = \frac{u+iv}{\sqrt{u^2+v^2}} = \exp\left[i\phi(u,v)\right]. \tag{8}$$

Here the phase ϕ is the polar angle in frequency space. The major influence in the conceptual and mathematical development of our spiral phase formalism has been the research on optical vortices. There are deep connections mainly related to the Fourier property of far-field diffraction patterns.[48-51] Spiral phase-plates or holograms in the Fourier plane are analogous to the Fourier multipliers of singular integrals. The phase spiral is also consistent with definitions of the 2-D Riesz transform represented by a complex quantity instead of a 2-vector. Figure 2 shows a representation of the principal value (p.v.) of the spectral polar angle $\phi(u,v)$. The 2π discontinuity in the phase p.v. $\phi(u,v)$ is unimportant because the complex exponential in equation (8) is continuous everywhere (except the origin). Our reason for using the function S is that it has the following properties:

i.) It has odd radial symmetry (so all sines convert to cosines and vice versa),

ii.) It only contains a single point discontinuity (maintaining circular symmetry),

iii.) There is no radial variation of magnitude or phase with radius, and the magnitude is unity, hence ensuring scale invariance,

iv.) The relative angular variation is constant so that it has uniform rotational properties.

This spiral phase Fourier multiplier is applied to a fringe pattern with its offset removed:[52]:

$$g(x,y) = f(x,y) - a(x,y) = b(x,y)\cos\left[\psi(x,y)\right]. \tag{9}$$

Hence the ideal quadrature function (assuming suitably band-limited amplitude and phase[53]) would be

$$\hat{g}(x,y) = -b(x,y)\sin\left[\psi(x,y)\right] \tag{10}$$

and the 2-D complex fringe pattern[54]

$$g - i\hat{g} = b\exp\left[i\psi\right]. \tag{11}$$

If we have a fringe pattern image $g(x,y)$ which has a unique orientation angle $\beta(x,y)$ associated with each point as shown in figure 3(a), then we find that our Fourier spiral phase operator has the following effect on the fringe pattern:

$$\mathrm{F}^{-1}\left\{\exp\left[i\phi(u,v)\right]\mathrm{F}\left\{g(x,y)\right\}\right\} \cong i\exp\left[i\beta(x,y)\right]b(x,y)\sin\left[\psi(x,y)\right] \tag{12}$$

The heuristic derivation of this important result is as follows. If we consider the Fourier transform of the localised fringe pattern in figure 3(a), then we obtain a distribution shown in figure 3(b). If we try to localise the pattern to a small region then the lobes in figure 3(b) become larger. The formal mathematical description of this process, utilising the method of stationary phase, is described in paper II. We ignore here the uncertainty principle which limits localising the fringes and the fringe lobes simultaneously. A cosine fringe pattern will give two lobes with the same polarity. Multiplying the lobes by the spiral phase will change the lobes to opposite polarity and introduce a phase factor $\exp(i\beta)$. It is well known that changing lobe polarity changes a cosine into a negative sine, and the orientational phase then appears as a factor on top of this quadrature effect.

The above Fourier multiplication is also equivalent to a 2-D convolution of the image function with a spatial spiral phase kernel function $s(x,y)$

$$\mathrm{F}^{-1}\left\{\exp\left[i\phi(u,v)\right]\mathrm{F}\left\{g(x,y)\right\}\right\} = g(x,y) ** s(x,y), \tag{13}$$

where the kernel function can be shown by general Fourier techniques to be a rather interesting spiral-phase, inverse-square function

$$s(x,y) = \frac{i(x+iy)}{\left(x^2+y^2\right)^{3/2}} = \frac{i\exp(i\theta)}{r^2}. \tag{14}$$

The spatial polar coordinates being defined as usual

$$\left.\begin{aligned} x &= r\cos\theta \\ y &= r\sin\theta \end{aligned}\right\}. \tag{15}$$

Equation (14) can also be interpreted in terms of the 2-D Riesz kernels[29]

$$\begin{aligned} \mathrm{F}^{-1}\left\{-i\frac{u}{q}\right\} &= \frac{x}{r^3} \\ \mathrm{F}^{-1}\left\{-i\frac{v}{q}\right\} &= \frac{y}{r^3}. \end{aligned} \tag{16}$$

The convolution kernel approach may be important for efficient implementations of the spiral phase transformation.

We have defined an orientational phase factor $\exp\left[i\beta(x,y)\right]$ which is simply related to the fringe angle $\beta(x,y)$. The Fourier spiral phase approximation is derived by considering the Fourier components of localised fringes and is valid for suitably smoothly varying parameters (the local simplicity constraint[39]). The accuracy is better than one percent for typical patterns where the fringe radius of curvature is greater than the fringe spacing. In fact equation (12) can actually be used to define $\beta(x,y)$, but we take an alternative approach in the following examples. Orientation estimators are of great interest in human and computer vision, with some reliable methods currently available.[39] We use a special orientation estimator to find β_e, an estimator that does not flip 180º from fringe to fringe (ie. it is not a simple gradient estimator) and so maintains local continuity. Details of orientation estimation are provided in the appendix to paper II. The next step is to simply extract $\hat{g}$ and calculate the 2-D complex image:

$$g - i\hat{g} = g - \exp\left[-i\beta_e\right]\mathrm{F}^{-1}\left\{\exp\left[i\phi\right]\mathrm{F}\left\{g\right\}\right\}. \tag{17}$$

The process can be seen as combination of pure phase function multiplication in the space domain (x, y) and in the Fourier domain (u, v). The operator V{} defined by

$$\mathrm{V}\{g\} = -i\exp[-i\beta]\mathrm{F}^{-1}\{\exp[i\phi]\mathrm{F}\{g\}\} \tag{18}$$

we shall refer to as the vortex operator for brevity in the following text. The vortex operator has the following invariant properties: scale, translation, and rotation (for properly defined β). In essence the operator satisfies all the requirements of a hypothetical 2-D quadrature transform. The demodulation process defined by V{} can be said to be natural in the sense that $-b\sin(\psi)$ is the natural quadrature of $b\cos(\psi)$, for 2-D functions as well as 1D functions.

A particularly elegant solution arises for circular symmetric pattens such as circular fringes. In this case the orientation phase is just a single spiral but in the opposite sense of the Fourier spiral – the overall transform is then a double spiral (vortex) transform. As far as we know the direct demodulation of simple closed curve fringe patterns has not been presented before. We shall present examples in the next section. In fringe patterns with disjoint closed curve regions the question of global sign choice for the orientation is ambiguous and each separate region must have a sign allocated arbitrarily (or based on an additional global constraint). For clarity our examples will be restricted to simple (non-disjoint) closed curve patterns.

Application to two-dimensional fringe patterns

The first example using the vortex operator is a fringe pattern which could quite easily occur as a human fingerprint or as an optical interference pattern. Figure 4 is a flow chart of our proposed vortex operator algorithm. The direct algorithm is computationally efficient, requiring just two Fourier transforms and two multiplications (and an additional orientation estimation with comparable computational complexity). The output function is in quadrature to the input. All the examples are computed using the fast Fourier transform (FFT) on 128x128 discrete images without additional windowing operations. Notice how the Fourier transform magnitude contains a spectral lobe that is a continuous ring. Such rings have made previous attempts at direct Fourier transform demodulation impossible.[46, 55]

In figure 5 we show details of the input and output images compared to idealised quadrature pairs and alternative demodulation methods. The quadrant "Hilbert" transform[3, 14] has been included because it appeared recently in a problematic definition of the multi-dimensional analytic signal.[11] The vortex operator complex image is visually very close to the ideal, only failing close to the discontinuity at the centre. The half-plane Hilbert method fails seriously for any closed curve fringe pattern. The horizontal fringes are highly distorted in this case leading to a dark region in the estimated magnitude. The phase shows a local sign ambiguity and is also highly distorted in the transition region.[10] The quadrant Hilbert transform gives a slightly more isotropic estimate of the magnitude but fails rather badly with the phase estimate.[11]

In figure 6 we show a comparison of methods applied to the interference pattern from figure 4. This time the initial image has both amplitude and phase structure (AM-

FM). The input image also has uniform random noise added for realism (10% of peak signal, 100% of minimum signal). Again the vortex operator generates an estimated complex image that is visually close to the ideal. The actual error is in the range –28% to +10% in a region less than half of a fringe from the central discontinuity of the underlying conical phase function. Outside a region just two fringes from the centre the error drops below 3% and the closeness to the ideal magnitude is clear in figure 7. In contrast the half-plane Hilbert transform produces anisotropic magnitude and phase estimates with the usual visible artefacts as seen in figure 6. Note that these artefacts are typically very large (magnitude error in the range -98% to +35% for example) and widely dispersed as illustrated in figure 7.

4. An exact solution for circular symmetric patterns

Our equation defining the vortex operator derives from an approximation linking the sine and cosine components of a general fringe pattern. However, there is at least one simple circular symmetric function that transforms exactly using the vortex operator:

$$\mathrm{V}\left\{\mathrm{J}_0(\lambda r)\right\} = \mathrm{J}_1(\lambda r), \qquad 0 < \lambda \tag{19}$$

The Bessel functions asymptotically approach decaying sinusoids, for $\lambda r > 3$, which is essentially within one fringe period. The exact solution above suggests an inverse formula:

$$\mathrm{V}^{-1}\left\{\mathrm{J}_1(\lambda r)\right\} = \mathrm{J}_0(\lambda r), \text{ where } \mathrm{V}^{-1}\{g\} = i\,\mathrm{F}^{-1}\left\{\exp[-i\phi]\mathrm{F}\left\{\exp[i\beta]g\right\}\right\}. \tag{20}$$

However, such an inversion may be impractical in more general, non-circular symmetric cases. This is because the inverse requires that orientation estimation and multiplication take place before the Fourier spiral phase transformation. Consequently any errors in the orientation, especially discontinuities, will spread widely in the final result. The proposed forward algorithm does not have such a problem; any errors in the orientation estimate remain localised.

Summary

We have surveyed the literature on multi-dimensional Hilbert transforms and found that a number of groups have independently adopted a Riesz transform based definition (without necessarily recognising the Riesz transform). In other areas of research the directional, orthant based Hilbert transform definitions may have inhibited the evolution of isotropic forms. The proposed formalism for the vortex operator allows a quadrature transform and a complex "analytic" signal to be defined uniquely for any 2-D signals (images) which satisfy the local simplicity constraint. The constraint is in keeping with the restricted definition of instantaneous frequency and the analytic signal in one dimension.[56] We have demonstrated a new form of fringe pattern analysis using the vortex operator, which directly demodulates 2-D patterns previously considered impossible. We expect the vortex operator and the associated 2-D complex signal to have wide applications beyond the notable fringe pattern analysis presented here. The vortex operator may be implemented simply in an optical system using a spiral phase plate in the Fourier plane or the back focal plane of an imaging system allowing near instantaneous evaluation of quadrature functions and suggesting new optical imaging modes.

References

1 D. Gabor, "Theory of communications," Journal of the Institution of Electrical Engineers, **93**, 429-457, (1947).

2 S. Lowenthal, and Y. Belvaux, "Observation of phase objects by optically processed Hilbert transform," App. Phys. Lett. **11**, (2), 49-51, (1967).

3 H. Stark, "An extension to the Hilbert transform product theorem," Proc. IEEE **59**, 13591360, (1971).

4 J. K. T. Eu, and A. W. Lohmann, "Isotropic Hilbert spatial filtering," Opt. Comm. **9**, (3), 257-262, (1973).

5 J. Ojeda-Castanada, and E. Jara, "Isotropic Hilbert transform by anisotropic spatial filtering," App. Opt. **25**, (22), 4035-4038, (1986).

6 E. Peli, "Hilbert transform pairs mechanisms," Invest. Ophthalmol. Vis. Sci. **30 (ARVO Suppl.)**, 110, (1989).

7 A. W. Lohmann, E. Tepichin, and J. G. Ramirez, "Optical implementation of the fractional Hilbert transform for two-dimensional objects," App. Opt. **36**, (26), 6620-6626, (1997).

8 Y. M. Zhu, F. Peyrin, and R. Goutte, "The use of a two-dimensional Hilbert transform for Wigner analysis of 2-diemsional real signals," Sig. Proc. **19**, 205-220, (1990).

9 S. L. Hahn, Hilbert transforms in signal processing, Artech House, Inc., Norwood, MA, 1996.

10 J. P. Havlicek, J. W. Havlicek, and A. C. Bovik, "The Analytic Image,," IEEE International Conference on Image Processing, Santa Barbara,California, (1997),

11 T. Bülow, and G. Sommer, "A Novel Approach to the 2D Analytic Signal," CAIP'99, Ljubljana, Slovenia, (1999),

12 T. Bülow, "Hypercomplex Spectral Signal Representations for the Processing and Analysis of Images," PhD. Christian Albrechts University, 1999.

13 M. Craig, "Analytic Signals For Multivariate Data," Mathematical Geology **28**, (3), 315-329, (1996).

14 M. A. Fiddy, "The role of analyticity in image recovery," Image recovery: theory and application, ed. Stark, H. (Florida: Academic Press, 1987).

15 J. R. Fienup, and C. C. Wackerman, "Phase retrieval stagnation problems and solution," JOSA,A **3**, (11), 1897-1907, (1986).

16 Not surprisingly, a separable (ie orthant) definition of the multidimensional Hilbert transform only leads to separable solutions.

17 D. G. Fulton, and G. Y. Rainich, "Generalisations to higher dimensions of the Cauchy integral formula," Am. J. Math **54**, 235-241, (1932).

18 M. R. Arnison, C. J. Cogswell, N. I. Smith, P. W. Fekete, K.G. Larkin, "Using the Hilbert transform for 3D visualisation of differential interference contrast microscope images," J. Microsc. **199**, (1), 79-84, (2000).

19 K. G. Larkin, "Efficient nonlinear algorithm for envelope detection in white light interferometry," J. Opt. Soc. Am.,A **13**, (4), 832-843, (1996).

20 According to Ahmed Zayed (A. I. Zayed, Handbook of generalized function transformations, CRC, Boca Raton) the Hilbert transform was so named by G.H. Hardy after David Hilbert (1862-1943), who was the first to observe the conjugate functions now known as a Hilbert transform pair(in D. Hilbert, Grundzuge einer allgemeinen Theorie der linearen Integralgleichungen, 1912).

21 M. Riesz, "Sur les fonctions conjuguees," Mathematische Zeitschrift **27**, 218-244, (1927).

22 F. G. Tricomi, "Equazioni integrali contenenti il valor principale di un integrale doppio," Mathematische Zeitschrift **27**, 87-133, (1928).

23 G. Giraud, "Sur une classe generale d'equations a integrales principales," C.R. Acad.sci. Paris **202**, (26), 2124-2126, (1936).

24 S. G. Mikhlin, "Singular integral equations (in Russian)," Uspekhi Matematiceskich Nauk **3**, 29-112, (1948).

25 S. G. Mikhlin, Multidimensional singular integrals and integral equations, Pergamon, Oxford, 1965.

26 A. P. Calderon, and A. Zygmund, "On the existence of certain singular integrals," Acta Mathematica **88**, 85-139, (1952).

27 A. Zygmund, "On singular integrals," Rendiconti di matematica **16**, 468-505, (1957).

28 It seems that there may have been some dispute about the priority of some crucial results in the properties of multidimensional singular integrals (ie Mikhlin 1948 versus Calderon-Zygmund 1952).

29 E. M. Stein, Singular integrals and differentiability properties of functions, Princeton University Press, Princeton, N.J., 1970.

30 A. Carbery, "Harmonic analysis of the Calderon-Zygmund school, 1970-1993," Bulletin of the London mathematical Society **30**, 11-23, (1998).

31 M. N. Nabighian, "The analytic signal of two-dimensional magnetic bodies with polygonal cross-section: its properties and use for automated anomaly interpretation," Geophysics **37**, (3), 507-517, (1972).

32 M. N. Nabighian, "Toward a three-dimensional automatic interpretation of potential fiel data via generalized Hilbert transform: fundamental relations," Geophysics **49**, (6), 780-786, (1984).

33 W. M. Moon, A. Ushah, V. Singh, and B. Bruce, "Application of 2-D Hilbert transform in geophysical imaging with potential field data," IEEE Trans Geosci. Remote Sens. **26**, (5), 502-510, (1988).

34 A. E. Barnes, "Theory of 2-D Complex Seismic Trace Analysis," Geophysics **61**, (1), 264-272, (1996).

35 C. Pudney, and M. Robbins, "Surface extraction from 3D images via local energy and ridge tracing," DICTA, (1995), 240--245.

36 M. C. Morrone, and D. C. Burr, "Feature detection in human vision: a phase-dependent energy model," Proceedings of the Royal Society of London, B **235**, 221-245, (1988).

37 E. Peli, "Contrast in complex images," JOSA,A **7**, (10), 2032-2040, (1989).

38 P. Kube, and P. Perona, "Scale-space properties of quadratic feature detectors," IEEE Transactions on pattern analysis and machine intelligence **18**, (10), 987-999, (1996).

39 G. H. Granlund, and H. Knutsson, Signal processing for computer vision, Kluwer, Dordrecht, Netherlands, 1995.

40 R. Muller, and J. Marquard, "Die Hilberttransformation und ihre Verallgemeinerung in Optik und Bildeverarbeitung," Optik **110**, (2), 99-109, (1999).

41 J. A. Davis, D. E. McNamara, D. Cottrel, and J. Campos, "Image processing with the radial Hilbert transform: theory and experiments," Opt. Lett. **25**, (2), 99-101, (2000).

42 R. N. Bracewell, The Fourier transform and its applications, McGraw Hill, New York, 1978.

43 M. Takeda, H. Ina, and S. Kobayashi, "Fourier-transform method of fringe-pattern analysis for computer-based topography and interferometry," J. Opt. Soc. Am. **72**, (1), 156-160, (1982).

44 K. A. Nugent, "Interferogram analysis using an accurate fully automatic algorithm," App. Opt. **24**, (18), 3101-3105, (1985).

45 D. J. Bone, H.-A. Bachor, and R. J. Sandeman, "Fringe-pattern analysis using a 2-D Fourier transform," App. Opt. **25**, (10), 1653-1660, (1986).

46 T. Kreis, Holographic interferometry. Principles and methods, 1, Akademie Verlag GmbH, Berlin, 1996.

47 J. L. Marroquin, J. E. Figueroa, and M. Servin, "Robust Quadrature Filters," Journal of the Optical Society of America A-Optics & Image Science **14**, (4), 779-791, (1997).

48 J. F. Nye, and M. V. Berry, "Dislocations in wave trains," Proc. R. Soc. Lond. A. **336**, 165-190, (1974).

49 W. J. Condell, "Fraunhofer diffraction from a circular annular aperture with helical phase factor," JOSA,A **2**, (2), 206-208, (1985).

50 P. Coullet, L. Gil, and F. Rocca, "Optical Vortices," Opt. Comm. **73**, (5), 403-408, (1989).

51 I. V. Basistiy, V. Y. Bazhenov, M. S. Soskin, and M. V. Vasnetsov, "Optics of Light Beams With Screw Dislocations," Opt. Comm. **103**, (5-6), 422-428, (1993).

52 There are a number of ways to remove the offset. Low pass filtering is the simplest but often not the best method. In situations with multiple phase-shifted interferograms the difference of any two frames will have the offset nullified. Adaptive filtering methods can also provide more accurate offset removal.

53 A. H. Nuttall, "On the quadrature approximation to the Hilbert transform of modulated signals," IEEE Proceedings **54**, 1458-1459, (1966).

54 We shall refrain from calling this function the 2D analytic signal at present because there are several conflicting definitions of analyticity in multiple dimensions.

55 D. Malacara, M. Servin, and Z. Malacara, Interferogram analysis for optical testing, Marcel Dekker, New York, 1998.

56 L. Cohen, P. Loughlin, and D. Vakman, "On an ambiguity in the definition of the amplitude and phase of a signal," Sig. Proc. **79**, (3), 301-307, (1999).

Figure Legends

Figure 1. The half-plane signum function plotted as a function of frequency coordinates (u,v).

Figure 2. The spiral phase "signum" function exponent ϕ.

The principal value of the complex exponent $\phi(u,v)$ is shown in the range $\pm\pi$.

Figure 3(a). Definition of local orientation angle $\beta(x,y)$ for a locally simple fringe pattern.

Each point in the fringe pattern has a well-defined orientation angle.

Figure 3(b). The spectral sidelobes related to the local fringe pattern.

The lobes are located at a polar angle equal to the fringe normal angle.

Figure 4. Spiral phase algorithm for 2-D quadrature function estimation.

A purely real fringe pattern is converted to a purely imaginary quadrature pattern by the vortex operator. The pattern shown could be an interferogram or a fingerprint pattern, for example. The operation consists of a frequency domain spiral phase multiplication followed by a space domain orientation phase multiplication. An additional multiplication can convert the output to real.

Figure 5 Comparison of 2-D Hilbert transform methods for a simple image.

The complex image generated by three different methods are compared to the ideal. The vortex operator gives a result similar to the ideal magnitude and phase. Both the

half-plane and quarter-plane Hilbert operators give highly anisotropic estimates of magnitude and phase.

Figure 6 Comparison of 2-D Hilbert transform methods for AM-FM image.

The input image has both amplitude and frequency modulation with 10% uniform random noise added. The complex image generated by the vortex operator is visually (and numerically) close to the ideal. In contrast to this the half-plane Hilbert result shows gross errors in both magnitude and phase estimates.

Figure 7 Comparison of demodulated magnitudes for vortex operator and half plane Hilbert operator.

The vortex operator derives a close estimate of the complex image magnitude, failing only at discontinuities in the phase. The half-plane Hilbert operator derives a highly oscillatory estimate of the magnitude with substantial errors in all regions.

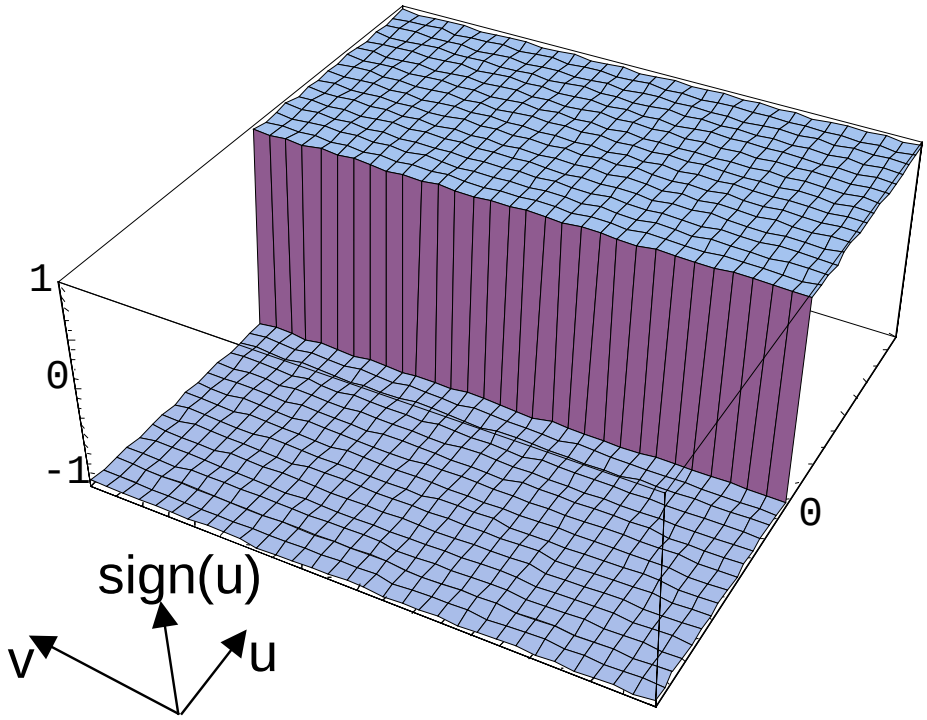

Figure 1

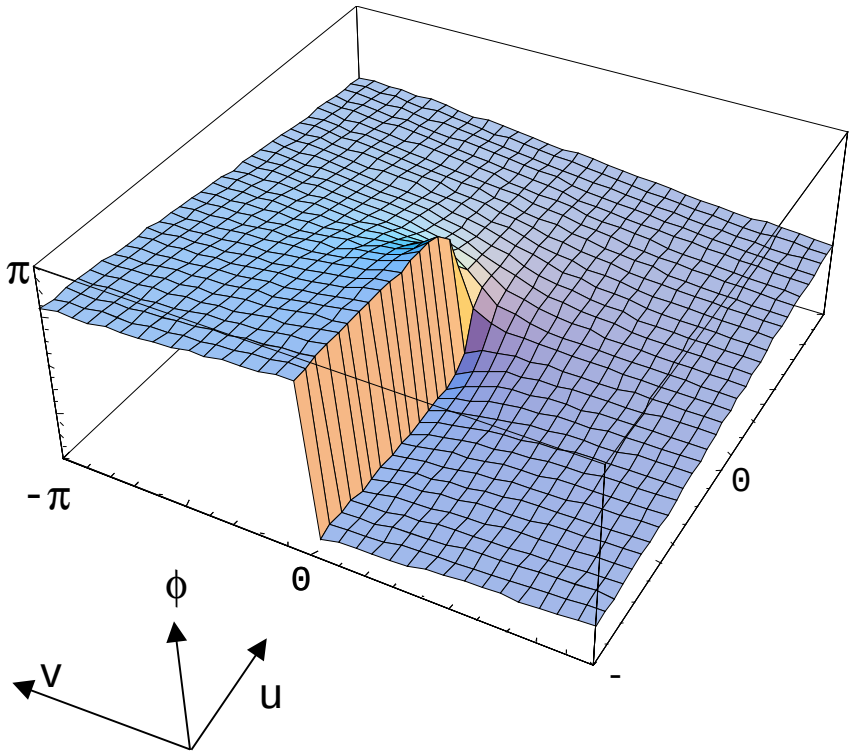

Figure 2

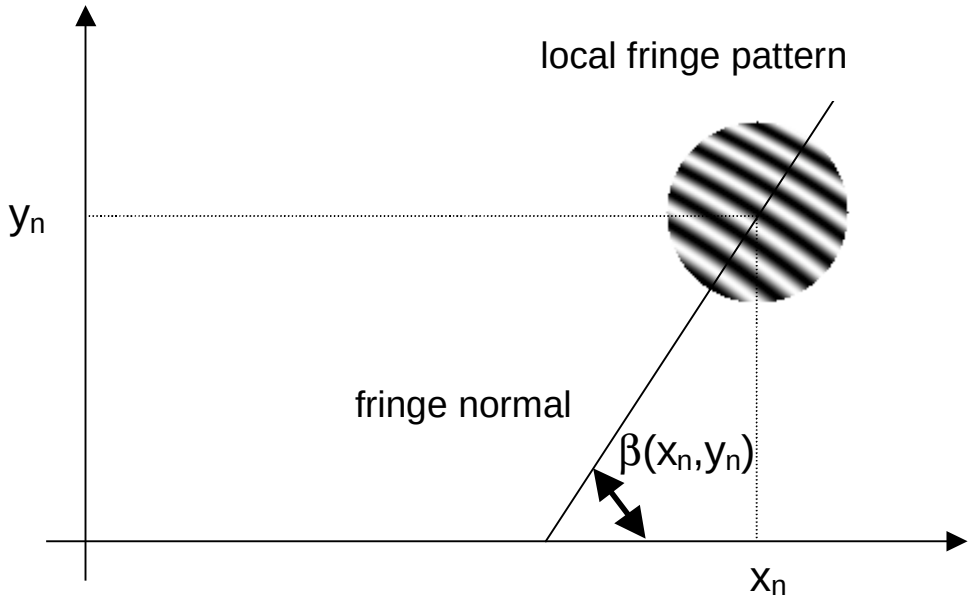

Figure 3(a)

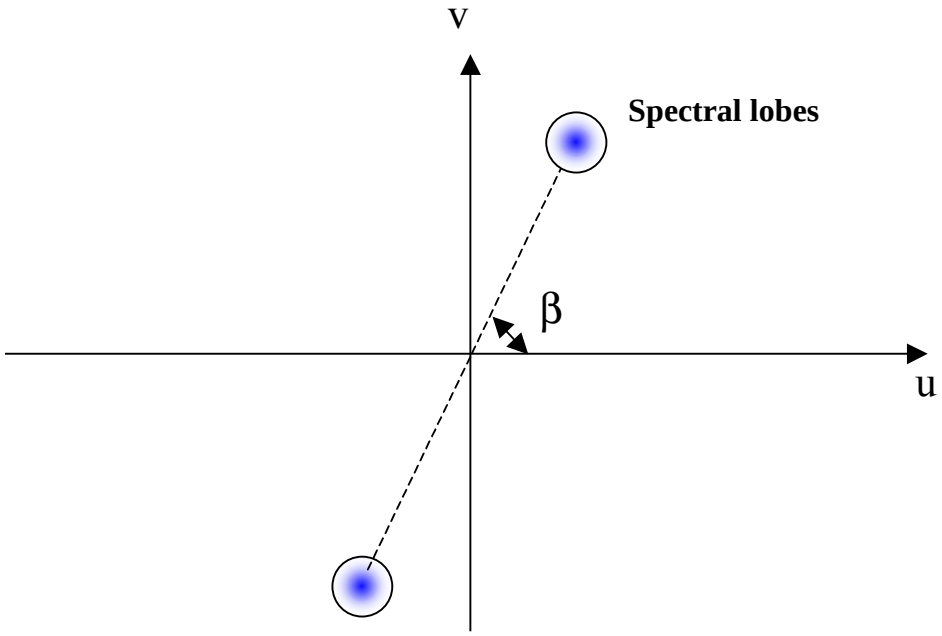

Figure 3(b)

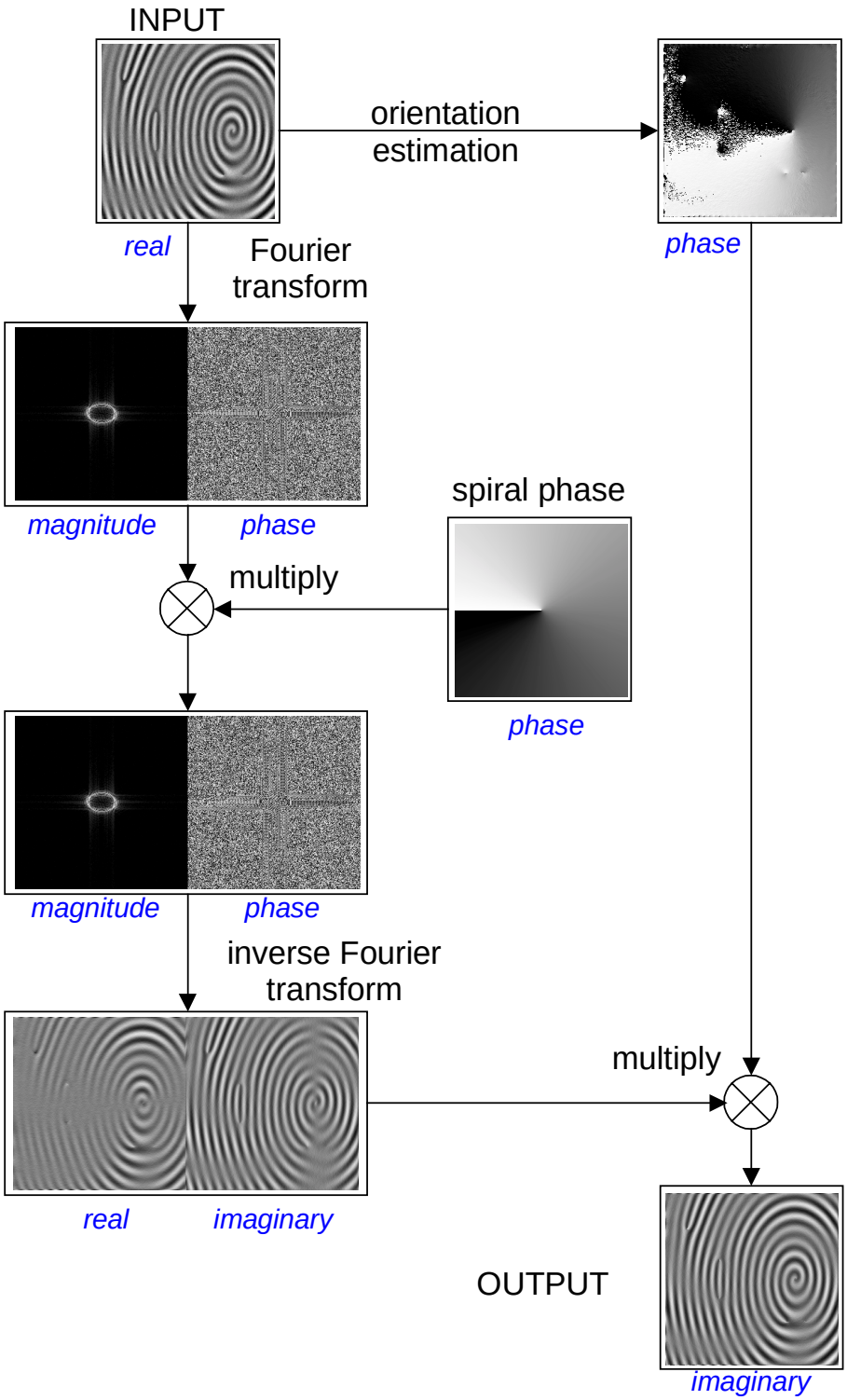
INPUT
orientation
estimation
real
Fourier
transform
phase
magnitude
phase
spiral phase
multiply
phase
magnitude
phase
inverse Fourier
transform
multiply
real
imaginary
OUTPUT
imaginary

Figure 4

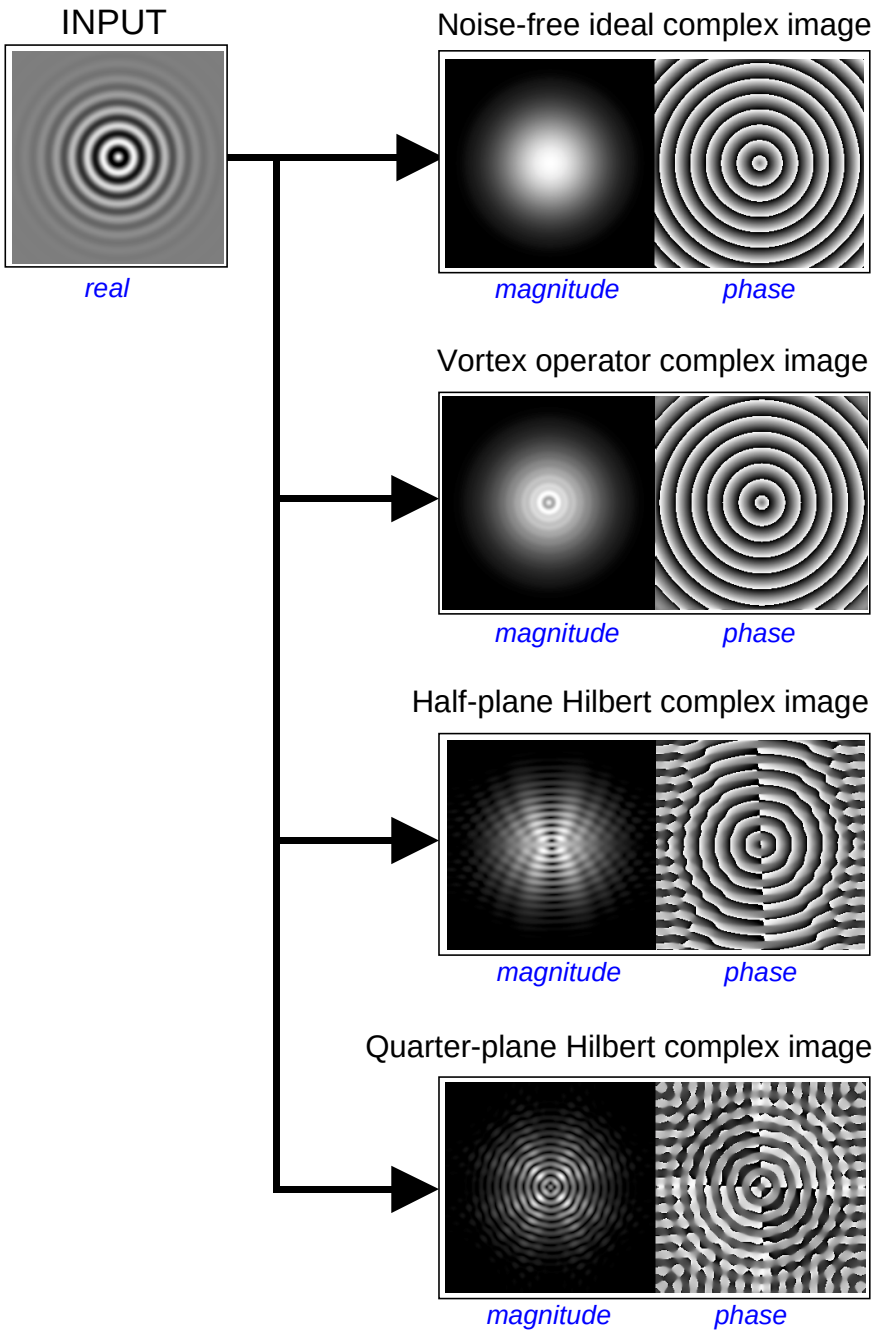
INPUT
real
Noise-free ideal complex image
magnitude
phase
Vortex operator complex image
magnitude
phase
Half-plane Hilbert complex image
magnitude
phase
Quarter-plane Hilbert complex image
magnitude
phase

Figure 5

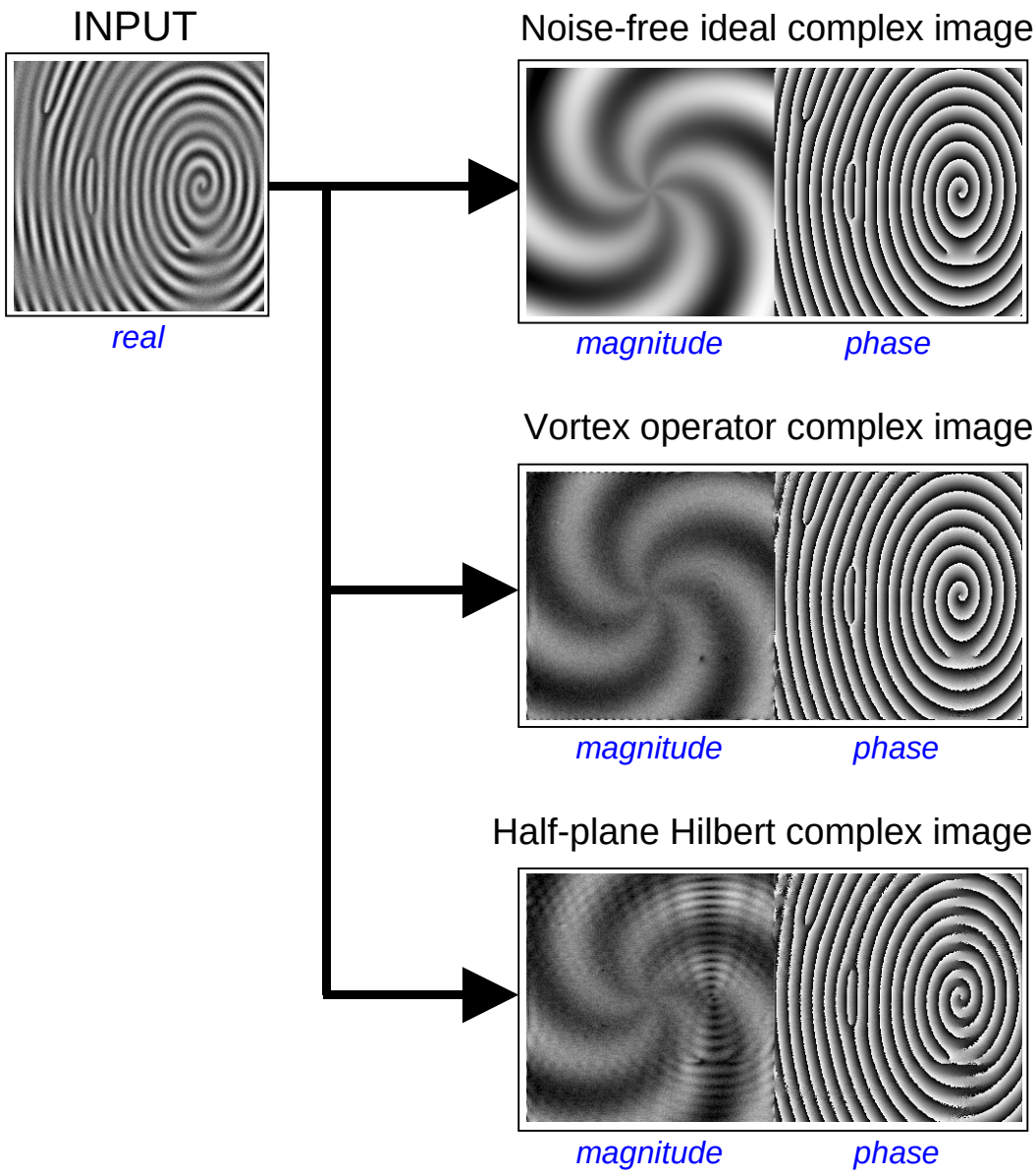
INPUT
real
Noise-free ideal complex image
magnitude
phase
Vortex operator complex image
magnitude
phase
Half-plane Hilbert complex image
magnitude
phase

Figure 6

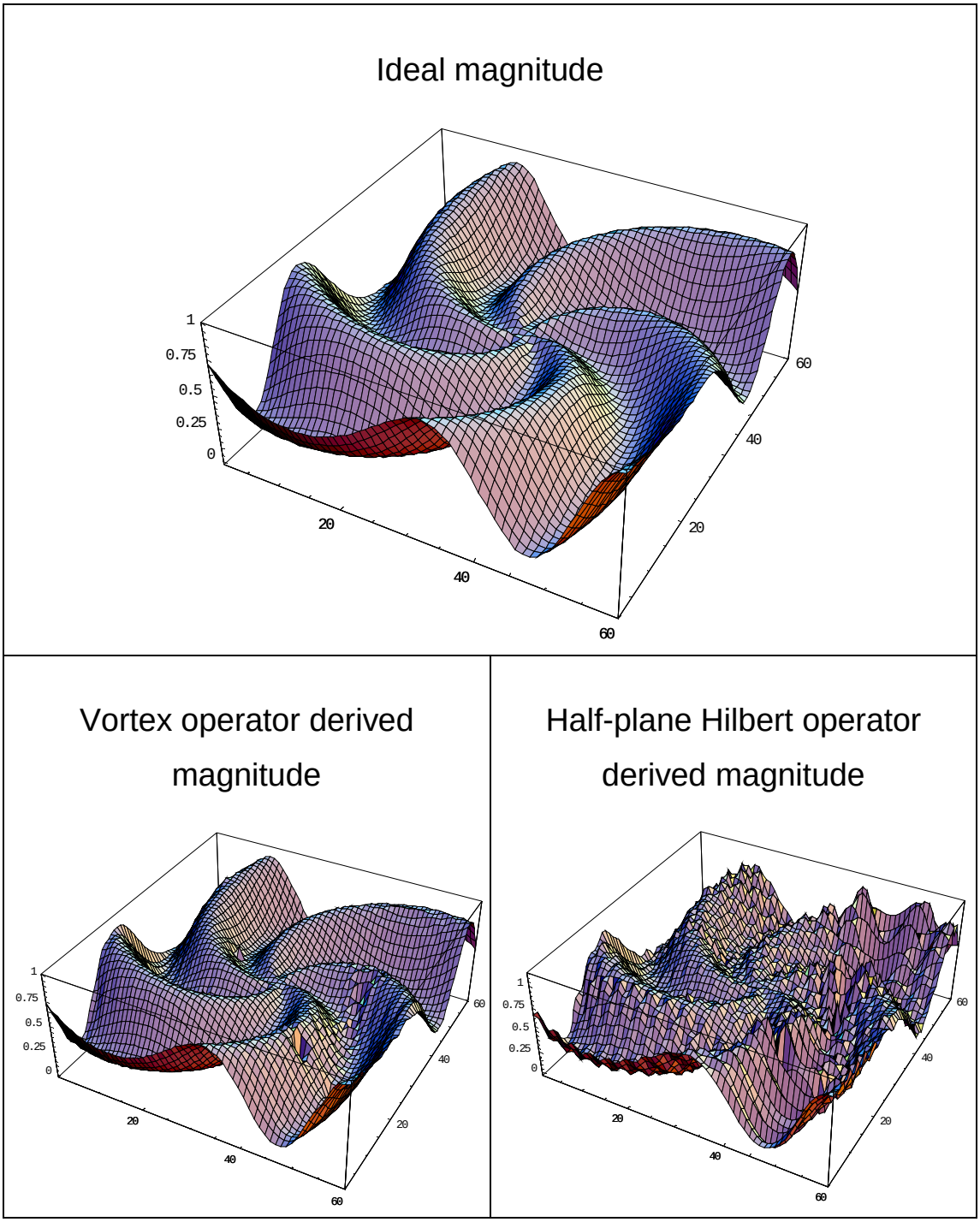
Ideal magnitude
1
0.75
0.5
0.25
0
20
40
60
20
40
60
Vortex operator derived magnitude
Half-plane Hilbert operator derived magnitude

Figure 7